

Alma Mater Studiorum Università di Bologna  
Archivio istituzionale della ricerca

Design-based stereological study of the guinea-pig (*Cavia porcellus*) cerebellum

This is the final peer-reviewed author's accepted manuscript (postprint) of the following publication:

*Published Version:*

De Silva, M., Sadeghinezhad, J., Nyengaard, J.R., Aghabalazadeh Asl, M., Saeidi, A., De Sordi, N., et al. (2021). Design-based stereological study of the guinea-pig (*Cavia porcellus*) cerebellum. JOURNAL OF ANATOMY, 239(2), 517-528 [10.1111/joa.13434].

*Availability:*

This version is available at: <https://hdl.handle.net/11585/846327> since: 2022-01-19

*Published:*

DOI: <http://doi.org/10.1111/joa.13434>

*Terms of use:*

Some rights reserved. The terms and conditions for the reuse of this version of the manuscript are specified in the publishing policy. For all terms of use and more information see the publisher's website.

This item was downloaded from IRIS Università di Bologna (<https://cris.unibo.it/>).  
When citing, please refer to the published version.

(Article begins on next page)

**Design-based stereological study of the guinea-pig (*Cavia porcellus*) cerebellum**

Running title: Guinea pig cerebellum stereology

Margherita De Silva<sup>1</sup>, Javad Sadeghinezhad<sup>2\*</sup>, Jens Randel Nyengaard<sup>3</sup>,  
Mahdi Aghabalazadeh Asl<sup>2</sup>, Ava Saeidi<sup>2</sup>, Nadia De Sordi<sup>1</sup>, Roberto  
Chiocchetti<sup>1</sup>, Annamaria Grandis<sup>1</sup>

<sup>1</sup>Department of Veterinary Medical Sciences (UNI EN ISO 9001:2008),  
University of Bologna, 40064, Ozzano dell'Emilia, Bologna, Italy

<sup>2</sup>Department of Basic Sciences, Faculty of Veterinary Medicine, University  
of Tehran, Tehran, Iran

<sup>3</sup>Core Centre for Molecular Morphology, Section for Stereology and  
Microscopy, Centre for Stochastic Geometry and Advanced Bioimaging,  
Aarhus University, Aarhus, Denmark

\*Corresponding author: Javad Sadeghinezhad

Email: [sadeghinezhad@ut.ac.ir](mailto:sadeghinezhad@ut.ac.ir)

## 21    **Abstract**

22            Guinea pigs have proved useful as experimental animal models in  
23    studying cerebellar anatomical and structural alterations in human  
24    neurological disease; however, they are also currently acquiring increasing  
25    veterinary interest as companion animals. The morphometric features of the  
26    normal cerebellum in guinea pigs have not been previously investigated  
27    using stereology. The objective of the present work was to establish normal  
28    volumetric and quantitative stereological parameters for cerebellar tissues  
29    in guinea pigs, by means of unbiased design-based stereology. Cerebellar  
30    total volume, grey and white matter volume fractions, molecular and  
31    granular layers volume fractions, cerebellar surface area, Purkinje cellular  
32    and nuclear volumes, and the Purkinje cell total count were stereologically  
33    estimated. For this purpose, cerebellar hemispheres from six adult male  
34    guinea pigs were employed. Isotropic, uniform random sections were  
35    obtained by applying the orientator method, and subsequently processed for  
36    light microscopy. The cerebellar total volume, the white and grey matter  
37    volume fractions, and the molecular and granular layer volumes were  
38    estimated using the Cavalieri's principle and the point counting system.  
39    The cerebellar surface area was estimated through the use of test lines;  
40    Purkinje cellular and nuclear volumes were analysed using the nucleator  
41    technique, whereas the Purkinje cell total count was obtained by means of

the optical disector technique. The mean  $\pm$  standard deviation (SD) total volume of a guinea-pig cerebellar hemisphere was  $0.11 \pm 0.01 \text{ cm}^3$ . The mean volumetric proportions occupied by the grey and white matters were, respectively,  $78.0 \pm 2.6\%$  and  $22.0 \pm 2.6\%$ , whereas their mean absolute volumes were found to be  $0.21 \pm 0.02 \text{ cm}^3$  and  $0.059 \pm 0.006 \text{ cm}^3$ . The volumes of the molecular and granular layers were estimated at  $112.4 \pm 20.6 \text{ mm}^3$  and  $104.4 \pm 7.3 \text{ mm}^3$ , whereas their mean thicknesses were calculated to be  $0.184 \pm 0.020 \text{ mm}$  and  $0.17 \pm 0.02 \text{ mm}$ . The molecular and granular layers accounted for  $40.7 \pm 3.9 \%$  and  $37.4 \pm 1.8 \%$  of total cerebellar volume, respectively. The surface area of the cerebellum measured  $611.4 \pm 96.8 \text{ mm}^2$ . Purkinje cells with a cellular volume of  $3210.1 \text{ } \mu\text{m}^3$  and with a nuclear volume of  $470.9 \text{ } \mu\text{m}^3$  had a higher incidence of occurrence. The mean total number of Purkinje cells for a cerebellar hemisphere was calculated to be  $253,090 \pm 34,754$ . The morphometric data emerging from the present study provide a set of reference data which might prove valuable as basic anatomical contribution for practical applications in veterinary neurology.

**Keywords:** Guinea pig, cerebellum, stereology, neuroanatomy, nervous system.

## 63    **Introduction**

64            The involvement of the cerebellum in motor coordination, balance  
65    and motor learning has been long and widely recognized (Brooks, 1984;  
66    Llinás and Welsh, 1993; Baillieux *et al.*, 2008; Lee *et al.*, 2015); however, a  
67    growing body of evidence involving neuroanatomical, neuroimaging and  
68    clinical studies indicates that it plays a significant role in non-motor  
69    behavioral-affective and cognitive functions, as well (Schmahmann and  
70    Caplan, 2006; Booth *et al.*, 2007; Molinari *et al.*, 2008; Cantalupo and  
71    Hopkins, 2010; Koziol *et al.*, 2011; De Smet *et al.*, 2013; Roostaei *et al.*,  
72    2014).

73            Design-based stereological techniques allow to efficiently acquire  
74    accurate and precise quantitative estimates of three-dimensional  
75    morphometric features of whole organs from measurements made on two-  
76    dimensional sections, by making use of statistical sampling and stochastic  
77    geometry principles (Boyce *et al.*, 2010).

78            Most stereological investigations on the cerebellum involving  
79    laboratory animals have been carried out on mice (Woodruff-Pak, 2006;  
80    Woodruff-Pak *et al.*, 2010; Wittmann and McLennan, 2011; Kennard *et al.*,  
81    2013; Song *et al.*, 2014), rats (Korbo *et al.*, 1993; Larsen *et al.*, 1993, 2000;  
82    Ragbetli *et al.*, 2007; Sonmez *et al.*, 2010) and rabbits (Akosman *et al.*,  
83    2011; Selçuk and Tıpırdamaz, 2020), but also on domestic animals such as

cats (Sadeghinezhad *et al.*, 2020), pigs (Jelsing *et al.*, 2006) and chicks (Tunç *et al.*, 2006). Apart from a stereological study performed on prenatal and neonatal guinea-pig cerebella following experimentally-induced intrauterine growth restriction (Mallard *et al.*, 2000), the morphometric features of the normal cerebellum in adult animals of this species have not been previously investigated using stereological techniques.

Guinea pigs (*Cavia porcellus*) have proved useful as experimental animal models in studying cerebellar anatomical and structural alterations in human neurological disease (Lev-Ram *et al.*, 1993; Furuoka *et al.*, 2011; Čapo *et al.*, 2015; Bennet *et al.*, 2017; Cumberland *et al.*, 2017), partly due to their high degree of neurological maturity at birth in relation to the short gestation period (Altman and Das, 1967; Hargaden and Singer, 2012; Silva *et al.*, 2016), which is important for clinical studies in human medicine. Indeed, the brain of newborn guinea pigs is singularly mature, and postnatal cerebellar neurogenesis is minimal in this precocial species (Altman and Das, 1967). It was observed that, as early as 45 days through gestation, cerebellar layers in guinea-pig fetuses were distinct and well developed, with easily identifiable Purkinje cells, and with the white and gray matters well differentiated both macro- and microscopically (Silva *et al.*, 2016). Moreover, cellular proliferation events in the cerebellum, unlike other rodents, are complete at birth in the guinea pig (Lossi *et al.*, 1997).

105           Recently, however, increasing interest has been addressed toward the  
106   clinical features, pathological changes and therapeutic resolution of  
107   neurological disorders of guinea pigs held as pet animals (Hollamby, 2009;  
108   Hawkins and Bishop, 2012). Most incidences of naturally-occurring  
109   cerebellar pathology reported in the literature for pet guinea pigs have an  
110   infectious etiology. Reported aetiological agents are, for instance, the  
111   lymphocytic choriomeningitis virus, leading to cerebellar hypoplasia with  
112   acute destruction of cortex folia and necrosis of granule and Purkinje cells  
113   (Monjan *et al.*, 1971; Hawkins and Bishop, 2012); *Toxoplasma gondii*,  
114   inducing granulomatous meningoencephalitis, foci of necrosis, and chronic  
115   cysts in the central nervous system (Brabb *et al.*, 2012; Gentz and  
116   Carpenter, 2012); and *Baylisascaris procyonis* larvae, causing progressive  
117   multifocal encephalomalacia and eosinophilic granulomatous inflammation  
118   of the cerebellum, midbrain and brainstem (Van Andel *et al.*, 1995).

119           In light of the above-listed scientific evidence, the objective of the  
120   present work was to establish normal volumetric and quantitative  
121   stereological parameters for cerebellar tissues in adult guinea pigs, by  
122   means of unbiased design-based stereology (Gundersen and Jensen, 1987;  
123   West, 1993; Boyce *et al.*, 2010). Specifically, the present study was  
124   designed to estimate cerebellar total volume, grey and white matter volume  
125   fractions, molecular and granular layers volume fractions [by using the

Cavalieri 's principle (Gundersen and Jensen, 1987)], estimate the cerebellar surface area (Schmitz and Hof, 2005), the total number of Purkinje cells [by employing the optical disector method (Gundersen, 1977; Sterio, 1984)], and the mean Purkinje cellular and nuclear volumes [through the use of the nucleator method (Gundersen *et al.*, 1988b)] in the guinea pig.

The morphometric data emerging from the present study provide an accurate set of reference data potentially valuable as basic anatomical contribution to the field of veterinary neurology in order to help implementing the development of the diagnosis and treatment of nervous diseases in the guinea pig.

## **Methods**

### **Animals and tissue preparation**

Six adult male pet guinea pigs, weighing  $569 \pm 64.9$  g, which spontaneously died of diseases other than those affecting the nervous system, were used for our research purposes following owners' permission. The animals did not present a history of neurological disease nor displayed pathological alterations of nervous tissues.

According to Directive 2010/63/EU of the European Parliament and of the 22 September 2010 Council on the protection of animals used for



scientific purposes, the Italian legislation (D. Lgs. n. 26/2014) does not require any approval by competent authorities or ethical committees, as this research did not influence any therapeutic decisions.

Guinea-pig cerebella were excised from the neurocranium in their entirety, each was divided into two halves, and then immersed in a 4% phosphate-buffered formaldehyde solution to enable tissue fixation. One hemisphere of each cerebellum was randomly chosen and weighed on a digital laboratory scale. The cerebellar hemispheres were routinely processed for light microscopic examination and subsequently embedded in paraffin.

#### **Tissue sampling and stereology**

The orientator method (Mattfeldt *et al.*, 1990; Nyengaard, 1999) was applied to obtain isotropic, uniform, random sections. In essence, each cerebellar hemisphere was embedded in a paraffin block, which was placed at the center of a circle with 90 equidistant divisions along the perimeter. A random number between 0 and 90 was looked up and the paraffin medium was cut along a line parallel to the direction of the selected number. The block was placed on its cut surface at the center of a second circle, with 96 nonequidistant divisions along its perimeter. The paraffin was cut along a line parallel to the direction of a random number ranging from 0 to 96, and the block was finally re-embedded in paraffin while placed on its cut

surface (Fig. 1). Consecutive 25 micrometer-thick sections were cut with a microtome at uniform constant intervals with a random start and until exhausting the organ. Every 25th section was collected using the principle of systematic uniform random sampling (Gundersen and Jensen, 1987), in order to acquire 12 to 15 sections per animal. Sections were then stained with Cresyl violet 0.1 % stain solution. A slide scanner (Optic lab H850, Plustek) was employed for capturing images from sections in order to enable the subsequent estimation of volumes and surface areas. A microscope (CX40, Olympus, Germany) equipped with an oil immersion objective ( $\times 100$ ), connected to a microcator (MT12, Heidenhain, Traunreut, Germany) and a digital camera (MB-225) was utilized for the estimation of Purkinje cells total cellular and nuclear volumes. Geometrical probes, necessary for the stereological analysis of each structural feature represented in each section (West, 1993), were produced using a dedicated software (ImageJ; <https://imagej.nih.gov>).

### **Estimation of total and fractional volumes**

The accurate estimation of cerebellar total volume was made possible by employing cerebellar weight and transforming it into a volume, and by applying the Cavalieri's estimator, taking therefore into account tissue shrinkage. Cerebellar shrinkage secondary to histological processing allows to obtain unbiased stereological estimations insensitive to

processing-dependent tissue deformations (Dorph-Petersen *et al.*, 2001).

The estimation of total volume starting from the weight of the cerebellum, was performed using the following formula:

$$V(\text{cerebellum}) = W(\text{cerebellum}) / \rho,$$

where  $\rho$  refers to the weight-to-volume ratio of cerebellar tissue.

The estimation of the total volume of the cerebellum through use of the Cavalieri principle was conducted by using the test point system (Fig. 2) and following the equation below (Howard and Reed, 1998):

$$V = \Sigma P \cdot SSF \cdot T \cdot (a/p)$$

where  $\Sigma P$  is the total number of points hitting the structure; SSF (1/25) represents the section sampling fraction; T (25  $\mu\text{m}$ ) is the section thickness and  $a/p$  (465,267  $\mu\text{m}^2$ ) refers to the area per point.

The fractional volume ( $V_v$ ) of cerebellar structures including white matter, grey matter, molecular and granular layers, was estimated using the following formula (Gundersen *et al.*, 1988a):

$$V_v(\text{structure}) = \Sigma P(\text{structure}) / \Sigma P(\text{cerebellum})$$

where  $\Sigma P(\text{structure})$  is the number of points hitting the white matter, gray matter, molecular and granular layers, and  $\Sigma P(\text{cerebellum})$  is the number of points hitting the cerebellum.

Lastly, in order to estimate the volume accounted for by each structure, each volume fraction was multiplied by the total volume of the

210 cerebellum.

## 211 **Estimation of surface area**

212 The surface density ( $S_v$ ) of the cerebellum was estimated by using  
213 test lines (Fig. 2b), and by employing the following formula (Howard and  
214 Reed, 1998):

$$215 \quad S_v = 2 \cdot \sum l / (\sum P \cdot l/p)$$

216 Where  $\sum l$  represents the total number of intersections between the outer  
217 surface of the cerebellum and the test lines,  $\sum P$  refers to the points hitting  
218 the molecular layer,  $l/p$  (658  $\mu\text{m}$ ) was the length of each test line associated  
219 to each point of the test grid.

220 Consequently, for estimating the surface area, surface density was multiplied  
221 by the volume of the molecular layer.

222 In addition, the thickness ( $T$ ) of the molecular and granular layers was  
223 calculated using the following formula (Andersen *et al.*, 2012):

$$224 \quad T(\text{layer}) = V(\text{layer}) / S(\text{layer})$$

225 where  $V$  is the volume and  $S$  is the surface area of each layer.

## 226 **Estimation of Purkinje cell total count**

227 The optical disector method was employed for the estimation of the  
228 Purkinje cell total number, and a motorized stage designed by Department  
229 of Anatomy, Faculty of Veterinary Medicine, of the University of Tehran,  
230 Tehran, Iran, was employed for the purpose. The microscopic fields were

selected by moving the microscope stage in the x and y directions for a constant distance spanning the entire section thickness. The unbiased counting frame principle was applied for counting the cells. The Purkinje cells whose nucleolus was located inside the counting frame or crossed the accepted lines were sampled, and those whose nucleolus came into focus within disector height were counted (Fig. 3).

The numerical density of Purkinje cells was calculated using the following formula (Kristiansen and Nyengaard, 2012):

$$N_v (\text{Purkinje cells}) = [\Sigma Q^- / (a/f \times \Sigma P \times h)] \times t/BA$$

where  $\Sigma Q^-$  represents the total count of Purkinje cells,  $a/f$  ( $9895 \mu\text{m}^2$ ) is the area per frame,  $\Sigma P$  is the total number of frames,  $h$  ( $10 \mu\text{m}$ ) is the disector height,  $t$  is the sections mean thickness ( $18.5 \mu\text{m}$ ), measured for each microscopic field, and  $BA$  ( $25 \mu\text{m}$ ) is the block advance.

Finally, for the estimation of the total number of Purkinje cells, the numerical density was multiplied by the total volume of the cerebellum, estimated using the Cavalieri's principle.

#### **Estimation of mean Purkinje cellular and nuclear volumes**

To estimate the volumes of Purkinje cells and Purkinje cell nuclei, the nucleator technique was utilized (Gundersen *et al.*, 1988b). The volume of the sampled cells was measured by using the unbiased counting frame,

and following the formula (Gundersen *et al.*, 1988b):

$$V_n = 4\pi/3 \cdot l_n^3$$

Where  $l_n$  refers to the intercept length from the nucleolus to the border of the cytoplasm (for cellular volume), or to the border of the nucleus (for nuclear volume) of Purkinje cells.

### Estimation of the coefficient of error (CE)

The precision of the volume estimates, expressed in terms of CE, is related to the variability associated with systematic uniform random sampling (SURS) sampling and point counting of the estimator. The CE for the estimate of the volume (Gundersen and Jensen, 1987), surface area (Kroustrup and Gundersen, 1983) and Purkinje cell count (Braendgaard *et al.*, 1990) was calculated.

### Statistical analysis

All data are expressed as mean  $\pm$  standard deviation (SD). As for right-skewed distributions, a logarithmic scale was used for individual estimates of Purkinje cellular and nuclear volumes (Weber *et al.*, 1997).

### Results

All cerebella evaluated appeared normal both macroscopically and on histological examination, with all the microscopical structures being

272 distinctly identifiable and without any evidence of pathological processes.

273         The mean ( $\pm$ SD) weight of a guinea-pig cerebellar hemisphere was  
274  $0.285 \pm 0.028$  g. The mean volume of a guinea pig cerebellar hemisphere,  
275 calculated by dividing the cerebellar weight by its specific gravity, was  
276  $0.274 \pm 0.027$  cm<sup>3</sup>, while the value obtained by employing the Cavalieri's  
277 estimator, was  $0.110 \pm 0.015$  cm<sup>3</sup>. A  $61.34 \pm 5.39\%$  total cerebellar volume  
278 shrinkage, secondary to the process of paraffin embedding, was estimated.  
279 The relative volume fractions of the grey and white matters, expressed as a  
280 percentage of total cerebellar volume, were found to be  $78.06 \pm 2.66\%$  and  
281  $21.92 \pm 2.67\%$ , respectively. Their absolute volumes, on the other hand,  
282 were calculated to be  $0.21 \pm 0.02$  cm<sup>3</sup> for the grey matter, and  $0.060 \pm$   
283  $0.006$  cm<sup>3</sup> for the white matter. The separate and mean values for the  
284 above-mentioned parameters, are outlined in Table 1.

285         The surface area of the cerebellum measured  $611.4 \pm 96.8$  mm<sup>2</sup>. The  
286 volume of the molecular layer was estimated to be  $112.41 \pm 20.56$  mm<sup>3</sup>  
287 while that of the granular layer  $104.38 \pm 7.31$  mm<sup>3</sup>; the molecular and  
288 granular layers accounted for  $40.67 \pm 3.87\%$  and  $37.38 \pm 1.77\%$  of total  
289 cerebellar volume, respectively. The mean thickness of the molecular and  
290 granular layers was  $0.184 \pm 0.020$  mm and  $0.169 \pm 0.017$  mm, respectively.  
291 In Table 2 are shown the mean and individual data calculated for the above-  
292 mentioned criteria in the six guinea pigs.

The frequency distribution of the Purkinje cellular and nuclear volumes is plotted in Fig. 4. The Purkinje cell volumes were found to be ranging from 987 to 8246.8  $\mu\text{m}^3$ , of which cells with a volume of 3210.1  $\mu\text{m}^3$  had a higher (13.71%) incidence of occurrence. The estimated volume of Purkinje nuclei was found to be ranging between <117 and 1623.4  $\mu\text{m}^3$ , and nuclei with a volume of 470.9  $\mu\text{m}^3$  were the most frequently occurring ones (13.54%).

The mean total number of Purkinje cells for a cerebellar hemisphere was calculated to be  $253,090 \pm 34,754$  (Table 3).

The mean coefficient of error (CE) and coefficient of variation (CV), along with their ratio ( $\text{CE}^2/\text{CV}^2$ ), calculated for total cerebellar volume, grey and white matter volume fractions, granular and molecular layers volume fractions, cerebellar surface area, and total number of Purkinje cells are shown in Table 4.

## Discussion

The mean total volume of a guinea-pig cerebellar hemisphere estimated in the present study is consistent with that calculated in a previous work, which investigated the brain morphology of domestic guinea pigs through quantitative cytoarchitectonic measurements (Kruska, 2014). Cerebellar total volume has been previously assessed by



stereological techniques in other species such as humans, which exhibited a difference between sexes, with male cerebella measuring  $120.5 \pm 11.1 \text{ cm}^3$  in volume, while females  $105.9 \pm 11.2 \text{ cm}^3$  (Taman *et al.*, 2020). Cerebellar volume has also been stereologically estimated in rabbits (Karabekir *et al.*, 2014) and rats (Noorafshan *et al.*, 2018), presenting volumes of  $0.69 \pm 0.03 \text{ cm}^3$ , and  $0.080 \pm 0.004 \text{ cm}^3$  for each cerebellar hemisphere, respectively, but also in cats (Sadeghinezhad *et al.*, 2020), presenting a mean cerebellar hemisphere volume of  $2.06 \pm 0.29 \text{ cm}^3$ . When comparing total cerebellar volume (in  $\text{cm}^3$ ) in relation to body weight (in kg) in each species, it appears that the guinea pigs of the present study have a cerebellar volume to body weight ratio of 0.9, which is consistent with the 0.8 calculated for the rat (Noorafshan *et al.*, 2018), but greater than the 0.4 estimated for the rabbit (Karabekir *et al.*, 2014), and less than an approximate 1.7 for an adult individual of average weight (Taman *et al.*, 2020) and than the approximate 1.1 calculated for a medium-sized cat (Sadeghinezhad *et al.*, 2020).

The cerebellar weight to body weight ratio was 0.1 in the guinea pig study population, which is in line with an approximate 0.13 calculated for a medium-sized cat (Sadeghinezhad *et al.*, 2020). Cerebellar volumetric modifications have been correlated with physiological factors such as age, gender (Raz *et al.*, 1998), cognitive capability, but also with several

pathological neurological conditions such as Alzheimer's disease, schizophrenia and epilepsy in humans (Bottmer *et al.*, 2005; Sato *et al.*, 2007; Bas *et al.*, 2009; Andersen *et al.*, 2012). A study carried out on rats has also identified a correlation between maternal diabetes and a reduction of total cerebellar volume and thickness of all layers in the offspring (Hami *et al.*, 2016). Volumetric prediction of the cerebellum can therefore find a valuable use in further research on veterinary neurological disease affecting cognition.

The cerebellar gray and white matter volumes have also been stereologically estimated in other species. The total gray matter volume of human cerebella has been calculated to be 88.5 cm<sup>3</sup>, while that of the white matter 22.5 cm<sup>3</sup> (Andersen *et al.*, 2012). Cerebellar grey and white matter volumes were estimated to be  $1.46 \pm 0.24$  cm<sup>3</sup> and  $0.60 \pm 0.06$  cm<sup>3</sup>, respectively, for the cat (Sadeghinezhad *et al.*, 2020). When compared to the guinea pig and cat, the proportionally more voluminous grey matter in humans can be likely ascribed to their increased development of motor control, coordination, as well as cognitive functions. Moreover, it was noted that, in the early domesticated mammals such as the guinea pig, a decrease in total brain size, which is proportional to the level of encephalization of the species, along with a decrease in total cortex and areas responsible for processing sensory information and motor control,

such as the grey matter, occurred as a consequence of the domestication process, with, however, the cognitive functions not being affected by this change (Kruska, 2005; Kaiser *et al.*, 2015; Welniak-Kaminska *et al.*, 2019). The volumes of the grey and white matter calculated in the present study are markedly greater than those reported by Mallard *et al.* (2000) for neonatal guinea pigs, which is likely due to the large age and body weight discrepancy. The influence of the physiological process of aging on volumetric changes in the cerebellar gray and especially the white matter has been assessed in several studies (Jernigan *et al.*, 2001; Walhovd *et al.*, 2005). Several human neurological diseases affecting cognition have also been observed to cause volume losses of the cerebellar gray and white matters (Fennema-Notestine *et al.*, 2004; Anderson *et al.*, 2009), as evidence of the role that the cerebellum plays in cognition.

The mean volumes of the molecular and granular layers in the guinea pig cerebellum estimated in the present work are significantly greater than the corresponding values reported by Mallard *et al.* (2000) for neonatal guinea pigs, and, comparing the two studies, the volumes of the two layers are apparently not proportionally related to body weight. The mean corresponding volumes referring to humans are 54.4 cm<sup>3</sup> for the molecular layer, and 37.9 cm<sup>3</sup> for the granular layer (Andersen, 2004). The mean

volume of the molecular and granular layers of the cerebellum of normal rats was reported to be 0.035 cm<sup>3</sup> and 0.024 cm<sup>3</sup>, respectively (Dortaj *et al.*, 2018). In cats' cerebella, the mean molecular layer volume had been reported to be 0.89 ± 0.16 cm<sup>3</sup>, while that of the granular layer 0.56 ± 0.10 cm<sup>3</sup> (Sadeghinezhad *et al.*, 2020). The relative proportions of the molecular and granular layers of the cerebellum in the different species seem to be conserved, thanks to the similar cerebellar microscopical anatomy. As a matter of fact, the histological examination of the guinea pig cerebella permitted the clear identification of the molecular, Purkinje and granular layers with their characteristic cellular populations. The conserved volumetric trend seems to be therefore related to function.

A stereological study carried out on intrauterine growth-restricted guinea pigs secondary to placental insufficiency in the second half period of pregnancy, has been seen to cause a reduction in the volume of the molecular and granular layers, as well as in that of the white matter in prenatal guinea-pig cerebella, therefore causing cognitive, motor and behavioral deficits in the post-natal life (Mallard *et al.*, 2000).

When analyzing the distribution of the thickness of the molecular and granular layers in the different subjects comprising our study population, it appears that the measurements are quite consistent and

regular, in contrast with what Sultan and Braitenberg (1993) had reported for smaller mammalian species. Andersen (2004) calculated a mean thickness of the molecular layer of  $590.00 \pm 0.08 \mu\text{m}$  and  $410.00 \pm 0.15 \mu\text{m}$  for the granular layer in human cerebella. Sadeghinezhad *et al.* (2020), on the other hand, calculated  $133.5 \pm 10.1 \mu\text{m}$  for the molecular layer and  $84.7 \pm 17.3 \mu\text{m}$  for the granular layer in cats' cerebella. Consistently with human and cats' cerebella, the molecular layer appears thicker than the granular, although not in a statistically significant manner; however, it seems that the thickness in guinea pigs is more uniformly-distributed between the two layers when compared to cats and humans' data. This can be explained by different physiological factors such as age. Indeed, a study carried out on cats' cerebella showed that aging causes an increase in granular layer thickness at the expense of that of the molecular layer (Zhang *et al.*, 2006).

With regard to the measurement of the cerebellar surface area, the ratio of cerebellar surface area to cerebellar weight in the different animals comprising the study population remains fairly constant, supporting the proportionality between cerebellar area and cerebellar weight hypothesized by Sultan and Braitenberg for larger mammals (1993), which is probably due, unlike other smaller mammalian species, to the equally constant distribution of grey matter thickness values in our guinea pig population. Further studies on larger population samples are needed to confirm this

418 finding. The average surface area of the human cerebellum has been  
419 previously estimated by different authors to be 550 cm<sup>2</sup> (Henery and  
420 Mayhew, 1989), 1027 cm<sup>2</sup> (Andersen *et al.*, 2012) and 1160 cm<sup>2</sup> (Andersen  
421 *et al.*, 1992). The human cerebellum, during evolution, underwent a  
422 significant expansion of its surface area both in absolute terms as well as in  
423 relation to the neocortex; this growth played a critical role in human  
424 cognitive development in comparison with other animals, given the role of  
425 the cerebellum in cognition (Barton and Venditti, 2014). In the animal  
426 kingdom, therefore, it is likely that the cerebellar surface area of highly  
427 encephalized species such as higher primates might show a greater  
428 development in comparison with mammals of a similar size. On the other  
429 hand, a mild but significant reduction in the total cerebellar area has been  
430 described in humans with advancing age, showing varying decline trends in  
431 the different vermian lobules (Raz *et al.*, 1998). A study carried out on  
432 experimentally vitamin C-deprived guinea pig fetuses has revealed a  
433 significant reduction in cerebellar surface area due to the obliteration of  
434 fissures and the fusion of opposing folia, resulting in a macroscopically-  
435 visible cerebellar dysplasia in terms of flattening of its surface, analogously  
436 to that observed in Lysencephaly Type 2 (Čapo *et al.*, 2015). The  
437 mentioned study is of clinical relevance in pet guinea pigs due to their  
438 natural incapability of endogenous vitamin C synthesis (Nishikimi *et al.*,

1992), analogously to humans, resulting in the necessity of its dietary supplementation, with the risk of developing vascular as well as neurological disease in case of deprivation.

Purkinje cells with a perikaryon volume of  $3210.1 \mu\text{m}^3$  and with a nuclear volume of  $470.9 \mu\text{m}^3$  were found to have the highest frequency of occurrence in the guinea pig cerebellum. Mean Purkinje cellular perikaryon volumes had been estimated to be  $12400 \mu\text{m}^3$  in humans (Korbo and Andersen, 1995),  $4900 \mu\text{m}^3$  (Korbo and Andersen, 1995) and  $5600 \mu\text{m}^3$  (Sørensen *et al.*, 2000) in rats,  $17600 \mu\text{m}^3$  in adult minipigs (Jelsing *et al.*, 2006),  $2207 \mu\text{m}^3$  in rabbits (Akosman *et al.*, 2011), and  $6994 \mu\text{m}^3$  in cats (Sadeghinezhad *et al.*, 2020). If considering a mean weight for an adult individual of each species, and calculating a ratio of Purkinje volume to body weight, these findings suggest a non-allometric correlation. Indeed, the mini-pig (Jelsing *et al.*, 2006) has a Purkinje volume to body weight ratio that is six times greater than that of humans (Korbo and Andersen, 1995), whereas rodents such as the rat (Sørensen *et al.*, 2000) and the guinea pig have, respectively, ratios that are 40 and 180 times proportionally greater than that of humans. The variability encountered might be explained by the different degrees of tissue shrinkage (Andersen *et al.*, 1992), by the immersion time of the tissue in the fixative (Jelsing *et al.*, 2006), by the degree of postnatal development of Purkinje perikaryon

volume (Jelsing *et al.*, 2006), or by different degrees of significance of Purkinje cell roles in motor, sensory and cognitive functions among the different species.

The mean total number of Purkinje cells calculated in the present work is consistent with the value reported for the whole cerebellum in a previous work carried out on neonatal guinea pigs, that is in the order of 500,000 (Mallard *et al.*, 2000). It has been demonstrated that the brain of newborn guinea pigs, species characterized by its precocity, presents a high degree of neurological maturity, and that postnatal cerebellar neurogenesis is minimal (Altman and Das, 1967). As a matter of fact, all cerebellar layers, including Purkinje cells, as well as white and gray matters, are well developed and differentiated as early as 45 days post conception (Silva *et al.*, 2016), and that all cerebellar cell proliferation events are entirely complete at birth in this species, unlike other similar rodents (Lossi *et al.*, 1997). In the adult mini-pig cerebellum, on the other hand, the total number of Purkinje cells was in the order of 2.8 million (Jelsing *et al.*, 2006). The numerosity of the Purkinje cell count in the above-mentioned study was, indeed, partially explained by a significant postnatal development in total Purkinje cell number and perikaryon volume, as it had also been demonstrated in rats (Altman and Bayer, 1978), humans (Miyata *et al.*, 1999), and cats (Vastagh *et al.*, 2005). The total number of Purkinje cells in



the whole adult rat cerebellum was estimated at around 320,000 cells (Sonmez *et al.*, 2010), which is markedly less than the value obtained for the guinea pig, and that could be explained by the complex heterogeneity of guinea pigs' Purkinje cells. It has been noted that Purkinje cells in the guinea pig cerebellum show a complex expression pattern of zebrin II, an immunohistochemical marker of cerebellar compartmental heterogeneity, showing three levels of zebrin II expression (Larouche *et al.*, 2003), as opposed to rats, where zebrin II expression only distinguishes two classes of Purkinje cells (Brochu *et al.*, 1990).

The hypothesis that less voluminous brains tend to have a higher cellular density than larger brains (Mwamengele *et al.*, 1993) does not seem to always be applicable, as is the case with the higher count of Purkinje cells in the guinea pigs comprising the present study when compared with the values reported for the rat (Sonmez *et al.*, 2010). Reports of acquired cerebellar degenerative disease in pet guinea pigs, mostly secondary to an infectious etiology, have been described in the literature, with ataxia and loss of voluntary motor control being common clinical signs, and meningoencephalitis and cerebellar cortical hypoplasia with necrosis of granule and Purkinje cells the principal histopathological findings (Monjan *et al.*, 1971; Van Andel *et al.*, 1995; Brabb *et al.*, 2012; Gentz and Carpenter, 2012; Hawkins and Bishop, 2012).

In conclusion, the present study represents the first detailed description of the morphometrical features of the guinea pig cerebellum using design-based stereological techniques. The reference morphometrical data provided for cerebellar structures might find a use as basic anatomical contribution to a greater understanding of neurological diseases when examining cerebellar pathology with relation to function in this exotic pet species of increasing veterinary interest. In addition, the present study might prove useful by providing a comparison with available data in humans and other mammals for future research investigating the basis of motor, cognitive and behavioral diseases in the different species.

#### **Conflict of interests**

The authors have no conflict of interests to declare.

#### **Author contributions**

M.D.S.: acquisition of data, data analysis/interpretation, drafting of the

manuscript; J.S.: concept/design, acquisition of data, data  
analysis/interpretation, critical revision and approval of the manuscript;  
J.R.N.: data analysis/interpretation, critical revision of the manuscript and  
approval of the article; M.A.A.: data analysis/interpretation; A.S.: data  
analysis/interpretation; N.D.S.: acquisition of data; R.C.: concept/design;  
critical revision of the manuscript and approval of the article; A.G.:  
acquisition of data, critical revision of the manuscript and approval of the  
article.

## References

Akosman, M.S., Gocmen-Mas, N. and Karabekir, H.S. (2011) Estimation  
of Purkinje cell quantification and volumetry in the cerebellum using a  
stereological technique. *Folia Morphologica (Warsz)*, **70**, 240-244.

Altman, J. and Bayer, S.A. (1978) Prenatal development of the cerebellar

541 system in the rat. I. Cytogenesis and histogenesis of the deep nuclei and the  
542 cortex of the cerebellum. *Journal of Comparative Neurology*, **179**, 23-48.  
543 doi: 10.1002/cne.901790104.

544 Altman J. and Das, G. (1967) Postnatal Neurogenesis in the Guinea  
545 pig. *Nature*, **214**, 1098–1101. <https://doi.org/10.1038/2141098a0>

546 Andersen, B. B. (2004) Reduction of Purkinje cell volume in cerebellum  
547 of alcoholics. *Brain Research*, **1007**, 10-18. doi:  
548 10.1016/j.brainres.2004.01.058

549 Andersen, B. B., Korbo, L. and Pakkenberg, B. (1992) A quantitative  
550 study of the human cerebellum with unbiased stereological techniques.  
551 *Journal of Comparative Neurology*, **326**, 549-460. doi:  
552 10.1002/cne.903260405

553 Andersen, K., Andersen, B.B. and Pakkenberg, B. (2012) Stereological  
554 quantification of the cerebellum in patients with Alzheimer's disease.  
555 *Neurobiology of Aging*, **33**, 197.e11-20.

556 Anderson, V. M., Fisniku, L. K., Altmann, D. R., Thompson, A. J and  
557 Miller, D. H. (2009) MRI measures show significant cerebellar gray matter  
558 volume loss in multiple sclerosis and are associated with cerebellar  
559 dysfunction. *Multiple Sclerosis Journal*, **15**, 811-817. doi:  
560 10.1177/1352458508101934

561 Baillieux, H., De Smet, H.J., Paquier, P.F., De Deyn, P.P. and Marien, P.  
562 (2008) Cerebellar Neurocognition: Insights into the bottom of the brain.  
563 *Clinical Neurology and Neurosurgery*, **110**, 763-773.

564 Barton, R. A. and Venditti, C. (2014) Rapid evolution of the cerebellum  
565 in humans and other great apes. *Current Biology*, **24**, 2440-1444. doi:  
566 10.1016/j.cub.2014.08.056

567 Bas, O., Acer, N., Mas, N., Karabekir, H. S., Kusbeci, O. Y. and Sahin,  
568 B. (2009) Stereological evaluation of the volume and volume fraction of  
569 intracranial structures in magnetic resonance images of patients with  
570 Alzheimer's disease. *Annals of Anatomy*, **191**, 186-195. doi:  
571 10.1016/j.aanat.2008.12.003

572 Bennett, G.A., Palliser, H.K., Shaw, J.C., Palazzi, K.L., Walker, D.W. and

573 Hirst, J.J. (2017) Maternal stress in pregnancy affects myelination and  
574 neurosteroid regulatory pathways in the guinea pig cerebellum. *Stress*, **20**,  
575 580-588.

576 Booth, J.R., Wood, L., Lu, D., Houk, J.C. and Bitan, T. (2007) The role  
577 of the basal ganglia and cerebellum in language processing. *Brain*  
578 *Research*, **1133**, 136-144.

579 Bottner, C., Bachmann, S., Pantel, J., Essig, M., Amann, M., Schad,  
580 L.R. and Schröder, J. (2005) Reduced cerebellar volume and neurological  
581 soft signs in first-episode schizophrenia. *Psychiatry Research*, **140**, 239–  
582 250.

583 Boyce, R.W., Dorph-Petersen, K.A., Lyck, L. and Gundersen, H.J.G.  
584 (2010) Design-based stereology: introduction to basic concepts and  
585 practical approaches for estimation of cell number. *Toxicologic Pathology*,  
586 **38**, 1011-1025.

587 Brabb, T., Newsome, D., Burich, A. and Hanes, M. (2012) Guinea pigs:  
588 infectious diseases. In: Suckow, M.A., Stevens, K.A. and Wilson, R.P.  
589 (Eds) The laboratory rabbit, guinea pig, hamster, and other rodents. San  
590 Diego, Elsevier, pp. 638-683.

591 Braendgaard, H., Evans, S.M., Howard, C.V. and Gundersen, H.J. (1990)  
592 The total number of neurons in the human neocortex unbiasedly estimated  
593 using optical disectors. *Journal of Microscopy*, **157**, 285-304.

594 doi: 10.1111/j.1365-2818.1990.tb02967.x.

595 Brooks, V.B. (1984) Cerebellar functions in motor control. *Human*  
596 *Neurobiology*, **2**, 251-260.

597 Brochu, G., Maler, L. and Hawkes, R. (1990) Zebrin II: A polypeptide  
598 antigen expressed selectively by purkinje cells reveals compartments in rat  
599 and fish cerebellum. *Journal of Comparative Neurology*, **291**, 538-552.  
600 doi: 10.1002/cne.902910405

601 Cantalupo, C. and Hopkins, W. (2010) The cerebellum and its  
602 contribution to complex tasks in higher primates: A comparative  
603 perspective. *Cortex*, **46**, 821-830.

604 Čapo, I., Hinić, N., Lalošević, D., Vučković, N., Stilinović, N.,  
605 Marković, J. and Sekulić, S. (2015) Vitamin C depletion in prenatal guinea  
606 pigs as a model of lissencephaly type II. *Veterinary Pathology*, **52**, 1263-  
607 1271.

608 Cavalieri, B. (1635) *Geometria Indivisibilibus Continuorum*. Nova  
609 *Quadam Ratione Promota*. Bononiae. Typis Clementis Fernoj. Reprinted  
610 as *Geometria degli Indivisibili*. Unione Tipografico-Editrice Torinese,  
611 Torino, Italy, 1966.

612 Cumberland, A.L., Palliser, H.K., Walker, D.W. and Hirst, J.J. (2017)  
613 Cerebellar changes in guinea pig offspring following suppression of  
614 neurosteroid synthesis during late gestation. *The Cerebellum*, **16**, 306-313.

615 De Smet, H.J., Paquier, P., Verhoeven, J. and Marien, P. (2013) The  
616 cerebellum: Its role in language and related cognitive and affective  
617 functions. *Brain and Language*, **127**, 334-342.

618 Dorph-Petersen, K.A., Nyengaard, J.R. and Gundersen, H.J. (2001)  
619 Tissue shrinkage and unbiased stereological estimation of particle number  
620 and size. *Journal of Microscopy*, **204**, 232-246. doi: 10.1046/j.1365-  
621 2818.2001.00958.x..

622 Dortaj, H., Yadegari, M., Hosseini Sharif Abad, M., Abbasi  
623 Sarcheshmeh, A. and Anvari, M. (2018) Stereological Method for  
624 Assessing the Effect of Vitamin C Administration on the Reduction of  
625 Acrylamide-induced Neurotoxicity. *Basic and Clinical Neuroscience*, **9**,  
626 27-34. doi: 10.29252/nirp.bcn.9.1.27

627 Fennema-Notestine, C., Archibald, S. L., Jacobson, M. W., Corey-  
628 Bloom, J., Paulsen, J. S., Peavy, G. M. *et al.* (2004) In vivo evidence of  
629 cerebellar atrophy and cerebral white matter loss in Huntington disease.  
630 *Neurology*, **63**, 989-995. doi: 10.1212/01.wnl.0000138434.68093.67

631 Furuoka, H., Horiuchi, M., Yamakawa, Y. and Sata, T. (2011)  
632 Predominant involvement of the cerebellum in guinea pigs infected with  
633 bovine spongiform encephalopathy (BSE). *Journal of Comparative*  
634 *Pathology*, **144**, 269-276.



635       Gentz, E. and Carpenter, J.W. (2012) Neurologic and musculoskeletal  
636       disease. In: Hillyer, E.V. and Quesenberry, K.E. (Eds) Ferrets, rabbits and  
637       rodents: clinical medicine and surgery. Philadelphia, WB Saunders, pp.  
638       220-226.

639       Gundersen, H.J.G. (1977) Notes on the estimation of the numerical  
640       density of arbitrary profiles: the edge effect. *Journal of Microscopy*, **111**,  
641       219-223.

642       Gundersen, H.J.G. and Jensen, E.B. (1987) The efficiency of systematic  
643       sampling in stereology and its prediction. *Journal of Microscopy*, **147**, 229-  
644       263.

645       Gundersen, H.J., Bendtsen, T.F., Korbo, L., Marcussen, N., Mallei, A.,  
646       Nielsen, K. *et al.* (1988a) Some new, simple and efficient stereological  
647       methods and their use in pathological research and diagnosis. *Acta*  
648       *Pathologica Microbiologica et Immunologica Scandinavica*, **96**, 379–394.

649       Gundersen, H.J., Bagger, P., Bendtsen, T.F., Evans, S.M., Korbo, L.,  
650       Marcussen, N. *et al.* (1988b) The new stereological tools: Disector,  
651       fractionator, nucleator and point sampled intercepts and their use in  
652       pathological research and diagnosis. *Acta Pathologica Microbiologica et*  
653       *Immunologica Scandinavica*, **96**, 857–881.

654       Hami, J., Vafaei-Nezhad, S., Ghaemi, K., Sadeghi, A., Ivar, G., Shojae, F.  
655       and Hosseini, M. (2016) Stereological study of the effects of maternal

656 diabetes on cerebellar cortex development in rat. *Metabolic Brain Disease*,  
657 **31**, 643-652. doi: 10.1007/s11011-016-9802-5

658 Hargaden, M. and Singer, L. (2012) Anatomy, Physiology, and Behavior.  
659 In: Suckow, M.A., Stevens, K.A. and Wilson, R.P. (eds) The laboratory  
660 rabbit, guinea pig, hamster, and other rodents. San Diego, Elsevier, pp. 575-  
661 602.

662 Hawkins, M.G. and Bishop, C.R. (2012) Disease problems of guinea  
663 pigs. In: Queesenberry, K.E. and Carpenter, J.W. (Eds) Ferrets, rabbits and  
664 rodents: clinical medicine and surgery. Philadelphia, Elsevier Saunders, p.  
665 307.

666 Hollamby, S. (2009) Rodents: neurological and musculoskeletal  
667 disorders. In: Keeble, E. and Meredith, A. (Eds) BSAVA manual of rodents  
668 and ferrets. Gloucester, BSAVA, pp. 161-168.

669 Howard, C.V. and Reed, M.G. (1998) Unbiased stereology. Three-  
670 dimensional measurement in microscopy. Bios Scientific Publishers,  
671 Oxford, pp. 107–123.

672 Henery, C. C. and Mayhew, T. M. (1989) The cerebrum and cerebellum  
673 of the fixed human brain: efficient and unbiased estimates of volumes and  
674 cortical surface areas. *Journal of Anatomy*, **167**, 167-180.

675 Jelsing, J., Gundersen, H.J., Nielsen, R., Hemmingsen, R. and  
676 Pakkenberg, B. (2006) The postnatal development of cerebellar Purkinje

677 cells in the Göttingen minipig estimated with a new stereological sampling  
678 technique--the vertical bar fractionator. *Journal of Anatomy*, **209**, 321-331.  
679 doi: 10.1111/j.1469-7580.2006.00611.x

680 Jernigan, T. L., Archibald, S. L., Fennema-Notestine, C., Gamst, A. C.,  
681 Stout, J. C., Bonner, J and Hesselink, J. R. (2001) Effects of age on tissues  
682 and regions of the cerebrum and cerebellum. *Neurobiology of Aging*, **22**,  
683 581-594. doi: 10.1016/s0197-4580(01)00217-2

684

685 Kaiser, S., Hennessy, M.B. and Sachser, N. (2015) Domestication affects  
686 the structure, development and stability of biobehavioural profiles.  
687 *Frontiers in Zoology*, **12**, S19. doi: 10.1186/1742-9994-12-S1-S19.

688 Karabekir, H.S., Akosman, M.S., Gocmen-Mas, N., Aksu, F., Edizer, M.,  
689 Lenger, O.F. and Turkmenoglu, I. (2014) The volume of experimental  
690 design cerebellum: stereological microanatomic study. *Journal of*  
691 *Craniofacial Surgery*, **25**, 1492-1494. doi:  
692 10.1097/SCS.0000000000000845.

693 Kennard, J.A., Brown, K.L. and Woodruff-Pak, D.S. (2013) Aging in the  
694 cerebellum and hippocampus and associated behaviors over the adult life  
695 span of CB6F1 mice. *Neuroscience*, **247**, 335-350.

696 Korbo, L. and Andersen, B. B. (1995) The distributions of Purkinje cell  
697 perikaryon and nuclear volume in human and rat cerebellum with the

698 nucleator method. *Neuroscience*, **69**, 151-158. doi: 10.1016/0306-  
699 4522(95)00223-6

700 Korbo, L., Andersen, B.B., Ladefoged, O. and Møller, A. (1993) Total  
701 numbers of various cell types in rat cerebellar cortex estimated using an  
702 unbiased stereological method. *Brain Research*, **609**, 262-268.

703 Koziol, L.F., Budding, D.E. and Chidekel, D. (2011) From movement to  
704 thought: executive function, embodied cognition, and the cerebellum. *The*  
705 *Cerebellum*, **11**, 505-525.

706 Kristiansen, S.L.B. and Nyengaard, J.R. (2012) Digital stereology in  
707 neuropathology. *Acta Pathologica Microbiologica et Immunologica*  
708 *Scandinavica*, **120**, 327-340.

709 Kroustrup, J.P. and Gundersen, H.J.G. (1983) Sampling problems in an  
710 heterogeneous organ: Quantitation of relative and total volume of  
711 pancreatic-islets by light-microscopy. *Journal of Microscopy*, **132**, 43–55.

712 Kruska, D.C.T. (2005) On the evolutionary significance of  
713 encephalization in some eutherian mammals: effects of adaptive radiation,  
714 domestication, and feralization. *Brain, Behavior and Evolution*, **65**, 73-108.  
715 doi: 10.1159/000082979.

716 Kruska, D.C.T. (2014) Comparative quantitative investigations on brains  
717 of wild caviars (*Cavia aperea*) and guinea pigs (*Cavia aperea f. porcellus*).

718 A contribution to size changes of CNS structures due to domestication.  
 719 *Mammalian Biology*, **79**, 230-239.

720 Larouche, M., Diep, C., Sillitoe, R.V. and Hawkes, R. (2003)  
 721 Topographical anatomy of the cerebellum in the guinea pig, *Cavia*  
 722 *porcellus*. *Brain Research*, **965**, 159-69. doi: 10.1016/s0006-  
 723 8993(02)04160-4.

724 Larsen, J.O., Skalicky, M. and Viidik, A. (2000) Does long-term physical  
 725 exercise counteract age-related Purkinje cell loss? A stereological study of  
 726 rat cerebellum. *Journal of Comparative Neurology*, **428**, 213-222.

727 Larsen, J.O., Tandrup, T. and Braendgaard, H. (1993) Number and size  
 728 distribution of cerebellar neurons estimated by the optical fractionator and  
 729 the vertical rotator. *Acta Stereologica*, **12**, 283-288.

730 Lee, K.H., Mathews, P.J., Reeves, A.M.B., Choe, K.Y., Jami, S.A.,  
 731 Serrano, R.E. and Otis, T.S. (2015) Circuit mechanisms underlying motor  
 732 memory formation in the cerebellum. *Neuron*, **86**, 529-540.

733 Lev-Ram, V., Valsamis, M., Masliah, E., Levine, S. and Godfrey, H.P.  
 734 (1993) A novel non-ataxic guinea pig strain with cerebrocortical and  
 735 cerebellar abnormalities. *Brain Research*, **606**, 325-331.

736 Llinás, R. and Welsh, J.P. (1993) On the cerebellum and motor learning.  
 737 *Current Opinion in Neurobiology*, **3**, 958-965.

738 Lossi, L., Marroni, P. and Merighi, P. (1997) Cell proliferation in the

739 cerebellar cortex of the rabbit and guinea pig. XXIst Congress of the  
740 European Association of Veterinary Anatomists. *Anatomia Histologia*  
741 *Embryologia*, **26**, 257.

742 Mallard, C., Loeliger, M., Copolov, D. and Rees, S. (2000) Reduced  
743 number of neurons in the hippocampus and the cerebellum in the postnatal  
744 guinea pig following intrauterine growth-restriction. *Neuroscience*, **100**,  
745 327-333.

746 Mattfeldt, T., Mall, G., Gharehbaghi, H. and Möller P. (1990) Estimation  
747 of surface area and length with the orientator. *Journal of Microscopy*, 159,  
748 301-317.

749 Molinari, M., Chiricozzi, F.R., Clausi, S., Tedesco, A.M., De Lisa, M.  
750 and Leggio, M.G. (2008) Cerebellum and detection of sequences: from  
751 perception to cognition. *The Cerebellum*, **7**, 611-615.

752 Monjan, A.A., Gilden, D.H., Cole, G.A. and Nathanson, N. (1971)  
753 Cerebellar hypoplasia in neonatal rats caused by lymphocytic  
754 choriomeningitis virus. *Science*, **171**, 194-196.

755 Miyata, M., Miyata, H., Mikoshiba, K. and Ohama, E. (1999)  
756 Development of Purkinje cells in humans: an immunohistochemical study  
757 using a monoclonal antibody against the inositol 1,4,5-triphosphate type 1  
758 receptor (IP3R1). *Acta Neuropathologica*, **98**, 226-32. doi:  
759 10.1007/s004010051073.

760 Mwamengele, G.L., Mayhew, T.M. and Dantzer, V. (1993) Purkinje cell  
761 complements in mammalian cerebella and the biases incurred by counting  
762 nucleoli. *Journal of Anatomy*, **183**, 155-60.

763 Nishikimi, M., Kawai, T. and Yagi, K. (1992) Guinea pigs possess a  
764 highly mutated gene for L-gulono-lactone oxidase, the key enzyme for L-  
765 ascorbic acid biosynthesis, missing in this species. *Journal of Biological*  
766 *Chemistry*, **267**, 21967-21972.

767 Noorafshan, A., Asadi-Golshan, R., Erfanizadeh, M. and Karbalay-  
768 Doust, S. (2018) Beneficial effects of olive oil on the rats' cerebellum:  
769 functional and structural evidence. *Folia Medica (Plovdiv)*, **60**, 454-463.  
770 doi: 10.2478/folmed-2018-0022

771 Nyengaard, J.R. (1999) Stereologic methods and their application in  
772 kidney research. *Journal of the American Society of Nephrology*, **10**, 1100-  
773 1123.

774 Ragbetli, M.C., Ozyurt, B., Aslan, H., Odaci, E., Gokcimen, A., Sahin,  
775 B. and Kaplan, S. (2007) Effect of prenatal exposure to diclofenac sodium  
776 on Purkinje cell numbers in rat cerebellum: A stereological study. *Brain*  
777 *Research*, **1174**, 130-135.

778 Raz, N., Dupuis, J.H., Briggs, S.D., McGavran, C. and Acker, J.D.  
779 (1998) Differential effects of age and sex on the cerebellar hemispheres and  
780 the vermis: a prospective MR study. *American Journal of Neuroradiology*,

781     **19**, 65-71.

782     Roostaei, T., Nazeri, A., Saharaian, M.A. and Minagar, A. (2014) The  
783     human cerebellum: a review of physiologic neuroanatomy. *Neurologic*  
784     *Clinics*, **32**, 859-869.

785     Sadeghinezhad, J., Aghabalazadeh Asl, M., Saeidi, A. and De Silva, M.  
786     (2020) Morphometrical study of the cat cerebellum using unbiased  
787     design-based stereology. *Anatomia Histologia Embryologia*, **49**, 788-797.  
788     doi: 10.1111/ahe.12583

789     Sato, N., Yagishita, A., Oba, H., Miki, Y., Nakata, Y., Yamashita, F. *et al.*  
790     (2007) Hemimegalencephaly: a study of abnormalities occurring outside  
791     the involved hemisphere. *American Journal of Neuroradiology*, **28**, 678-  
792     682.

793     Schmahmann, J.D. and Caplan, D. (2006) Cognition, emotion and the  
794     cerebellum. *Brain*, **129**, 290-292.

795     Schmitz C, Hof PR (2005) Design-based stereology in neuroscience.  
796     *Neuroscience* **130**:813-831.

797     Selçuk, M.L. and Tıpırdamaz, S. (2020) A morphological and  
798     stereological study on brain, cerebral hemispheres and cerebellum of New  
799     Zealand rabbits. *Anatomia Histologia Embryologia*, **49**, 90-96. doi:  
800     10.1111/ahe.12489

801     Silva, F.M.O., Alcantara, D., Carvalho, R.C., Favaron, P.O., Santos,



802 A.C., Viana, D.C. and Miglino, M.A. (2016). Development of the central  
 803 nervous system in guinea pig (*Cavia porcellus*, Rodentia, Caviidae).  
 804 *Pesquisa Veterinária Brasileira*, **36**, 753-760 doi: 10.1590/S0100-  
 805 736X2016000800013

806 Song, C.H., Bernhard, D., Hess, E.J. and Jinnah, H.A. (2014) Subtle  
 807 microstructural changes of the cerebellum in a knock-in mouse model of  
 808 DYT1 dystonia. *Neurobiology of Disease*, **62**, 372-380.

809 Sonmez, O.F., Odaci, E., Bas, O. and Kaplan, S. (2010) Purkinje cell  
 810 number decreases in the adult female rat cerebellum following exposure to  
 811 900MHz electromagnetic field. *Brain Research*, **1356**, 95-101. doi:  
 812 10.1016/j.brainres.2010.07.103

813 Sørensen, F. W., Larsen, J. O., Eide, R. and Schiønning, J. D. (2000)  
 814 Neuron loss in cerebellar cortex of rats exposed to mercury vapor: a  
 815 stereological study. *Acta Neuropathologica*, **100**, 95-100. doi:  
 816 10.1007/s004010051198

817 Sterio, D.C. (1984) The unbiased estimation of number and sizes of  
 818 arbitrary particles using the disector. *Journal of Microscopy*, **134**, 127-36.

819 Sultan, F. and Braitenberg, V. (1993) Shapes and sizes of different  
 820 mammalian cerebella. A study in quantitative comparative neuroanatomy.  
 821 *Journal für Hirnforschung*, **34**, 79-92.

822 Taman, F.D., Kervancioglu, P., Kervancioglu, A.S. and Turhan, B. (2020)

823 The importance of volume and area fractions of cerebellar volume and  
824 vermian subregion areas: a stereological study on MR images. *Child's*  
825 *Nervous System*, **36**, 165-171. doi: 10.1007/s00381-019-04369-9.

826 Tunç, A.T., Turgut, M., Aslan, H., Sahin, B., Yurtseven, M.E. and  
827 Kaplan, S. (2006) Neonatal pinealectomy induces Purkinje cell loss in the  
828 cerebellum of the chick: a stereological study. *Brain Research*, **1067**, 95-  
829 102. doi: 10.1016/j.brainres.2005.10.011

830 Van Andel, R.A., Franklin, C.L., Besch-Williford, C., Riley, L.K., Hook,  
831 R.R. Jr. and Kazacos, K.R. (1995) Cerebrospinal larva migrans due to  
832 *Baylisascaris procyonis* in a guinea pig colony. *Laboratory Animal Science*,  
833 **45**, 27-30.

834 Vastagh, C., Víg, J., Takács, J. and Hámori, J. (2005) Quantitative  
835 analysis of the postnatal development of Purkinje neurons in the  
836 cerebellum of the cat. *International Journal of Developmental*  
837 *Neuroscience*, **23**, 27-35. doi: 10.1016/j.ijdevneu.2004.09.005.

838 Walhovd, K. B., Fjell, A. M., Reinvang, I., Lundervold, A., Dale, A. M.,  
839 Eilertsen, D. E. *et al.* (2005) Effects of age on volumes of cortex, white  
840 matter and subcortical structures. *Neurobiology of Aging*, **26**, 1261-1270.  
841 doi: 10.1016/j.neurobiolaging.2005.05.020

842 Weber, U.J., Bock, T., Buschard, K. and Pakkenberg, B. (1997) Total  
843 number and size distribution of motor neurons in the spinal cord of normal

844 and EMC-virus infected mice—a stereological study. *Journal of Anatomy*,  
845 **191**, 347-353.

846 Welniak–Kaminska, M., Fiedorowicz, M., Orzel, J., Bogorodzki, P.,  
847 Modlinska, K., Stryjek, R. *et al.* (2019) Volumes of brain structures in  
848 captive wildtype and laboratory rats: 7T magnetic resonance in vivo  
849 automatic atlas-based study. *PLoS One*, **14**, e0215348. doi:  
850 10.1371/journal.pone.0215348

851 West, M.J. (1993) New stereological methods for counting neurons.  
852 *Neurobiology of Aging*, **14**, 275-285.

853 Wittmann, W. and McLennan, I.S. (2011) The male bias in the number of  
854 Purkinje cells and the size of the murine cerebellum may require Müllerian  
855 Inhibiting Substance/Anti-Müllerian Hormone. *Journal of*  
856 *Neuroendocrinology*, **23**, 831-838.

857 Woodruff-Pak, D.S. (2006) Stereological estimation of Purkinje neuron  
858 number in C57BL/6 mice and its relation to associative learning.  
859 *Neuroscience*, **141**, 233-243.

860 Woodruff-Pak, D.S., Foy, M.R., Akopian, G.G., Lee, K.H., Zach, J.,  
861 Nguyen, K.P.T. *et al.* (2010) Differential effects and rates of normal aging  
862 in cerebellum and hippocampus. *Proceedings of the National Academy of*  
863 *Sciences*, **107**, 1624-1629.

864 Zhang, C., Hua, T., Zhu, Z. and Luo, X. (2006) Age-related changes of

865 structures in cerebellar cortex of cat. *Journal of Biosciences*, **31**, 55-60. doi:

866 10.1007/bf02705235

867

868

869

870

871

872

873

874

875

876

877

878

879

880

881

882

883

884

885

886

887 Table 1. Stereological data for total volume of cerebellar hemisphere and  
888 proportional volume of gray matter and white matter in six guinea pigs.

889

890

Animals	Cerebellum weight (g)	Total volume of cerebellum (weight/specific gravity) (cm <sup>3</sup> )	Total volume of cerebellum (Cavalieri estimator) (cm <sup>3</sup> )	Shrinkage (%)	Gray matter		White matter	
					Volume fraction (%)	Volume (cm <sup>3</sup> )	Volume fraction (%)	Volume (cm <sup>3</sup> )
1	0.257	0.247	0.117	54.47	75.94	0.1875	24.05	0.0594
2	0.282	0.271	0.118	58.15	80.42	0.2179	19.57	0.0530
3	0.298	0.286	0.117	60.73	77.60	0.2219	22.39	0.0640
4	0.263	0.252	0.079	69.96	78.64	0.1981	21.35	0.0538
5	0.280	0.269	0.112	60	74.37	0.2000	25.62	0.0689
6	0.335	0.322	0.118	64.77	81.42	0.2621	18.57	0.0597
Mean±SD	0.285±0.028	0.274±0.027	0.110±0.015	61.34±5.39	78.06±2.66	0.2145±0.0266	21.92±2.66	0.0598±0.0060

891

892

893

894

895

896

897

898

899

900

901

902

903

904

905

906

907

908

909

910

911

912

913

914

915

916 Table 2. Stereological data for surface area, volume and thickness of  
 917 molecular and granular layers in cerebellar hemisphere in six guinea pigs.

918

919

Animals	1	2	3	4	5	6	Mean±SD
Surface area (mm <sup>2</sup> )	486.066	555.984	630.003	627.302	592.925	776.140	611.40±96.8
Volume fraction of molecular layer (%)	40.28	42.24	39.3	41.63	34.42	46.19	40.67±3.87
Volume of molecular layer (mm <sup>3</sup> )	99.4	114.4	112.3	104.9	92.5	151.0	112.41±20.56
Volume fraction of granular layer (%)	35.65	38.18	38.29	37.01	39.94	35.23	37.38±1.77
Volume of granular layer (mm <sup>3</sup> )	88.0	103.4	109.5	93.2	107.4	113.4	104.38±7.31
Thickness of molecular layer (mm)	0.204	0.205	0.178	0.167	0.156	0.194	0.184±0.020
Thickness of granular layer (mm)	0.181	0.185	0.173	0.148	0.181	0.146	0.169±0.017

920

921

922

923

924

925

926

927

Table 3. Stereological data for numeral density and total number of Purkinje cells in cerebellar hemisphere in six guinea pigs.

Animals	1	2	3	4	5	6	Mean±SD
Numeral density (cells/mm <sup>3</sup> )	2532	2413	2215	2546	2197	1986	2314.833 ± 220.099
Total number	296010	284380	258570	200660	245280	233640	253090 ± 34754

959

960

961 Table 4. The mean coefficient of error (CE) and coefficient of variation

	Total volume	Grey matter volume	White matter volume	Granular layer volume	Molecular layer volume	Surface area	Total number of Purkinje cells
CE	0.016	0.080	0.050	0.033	0.031	0.0162	0.080
CV	0.140	0.123	0.101	0.096	0.182	0.158	0.137
$CE^2/CV^2$	0.013	0.423	0.252	0.121	0.029	0.479	0.346

962 (CV) of stereological analysis of guinea pig cerebellum (n=6)

963

964

965

966

967

968

969

970

971

972

973

974

975

976

977

978



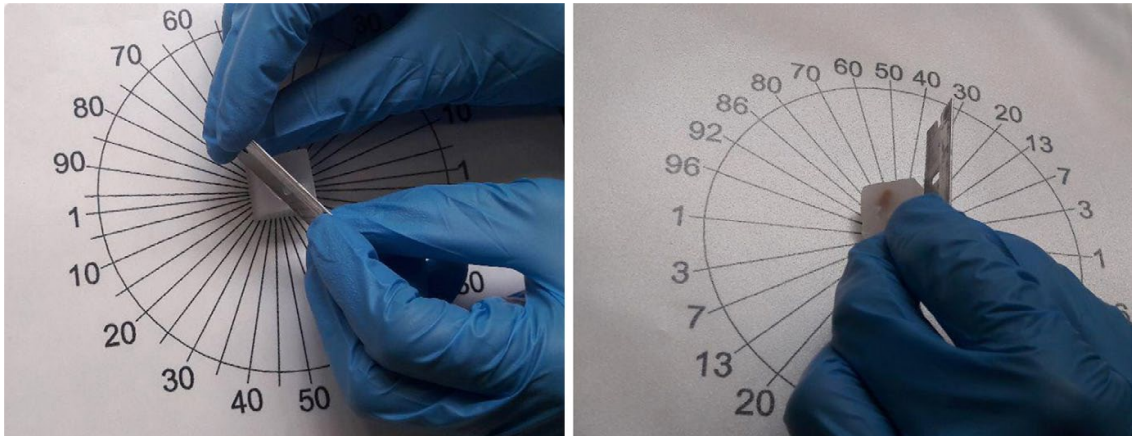


**Figure 1.** Isotropic, uniform random sections of the guinea-pig cerebellar hemispheres were obtained by applying the orientator method. (a): A randomly chosen cerebellar hemisphere for each animal was embedded in a paraffin block and placed at the centre of a circle with 90 equidistant divisions along the perimeter. A random number between 0 and 90 was looked up and the paraffin medium was cut along a line parallel to the direction of the selected number (here, 75). (b): The block was placed on its cut surface at the center of a second circle, with 96 nonequidistant divisions along its perimeter. The paraffin was cut along a line parallel to the direction of a random number ranging from 0 to 96 (here, 50), and the block was finally re-embedded in paraffin while placed on its cut surface, and consecutive 25  $\mu\text{m}$ -thick sections were cut with a microtome.

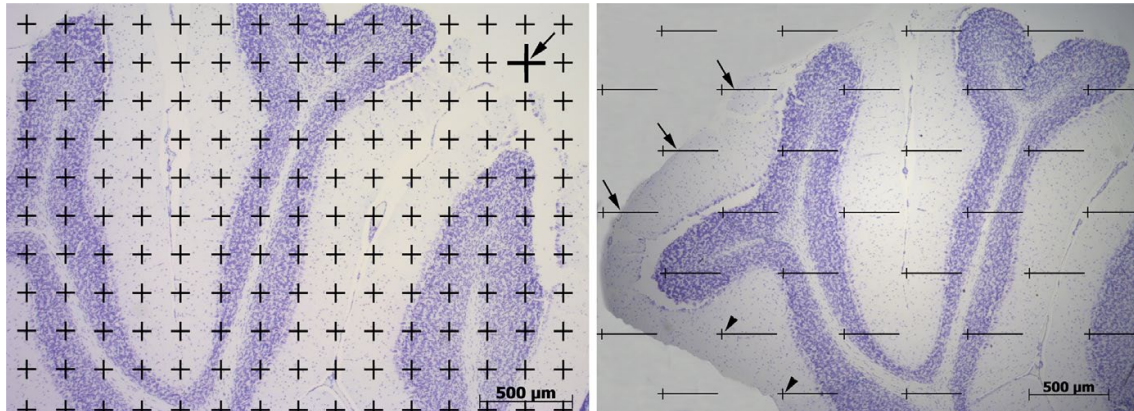


**Figure 2.** Estimation of cerebellar volume and surface area by employing the point-counting and the test-lines systems. (a): The volume of the cerebellar structures was estimated by randomly superimposing a point-counting probe onto each section. The upper right corner of each point (arrow) was taken as a reference for the count of the number of points hitting the region of interest. (b): The surface area of the cerebellum was estimated by superimposing test-lines onto each section. The arrowheads show two points hitting the molecular layer, whereas the arrows indicate the intersection between test lines with the outer cerebellar surface.

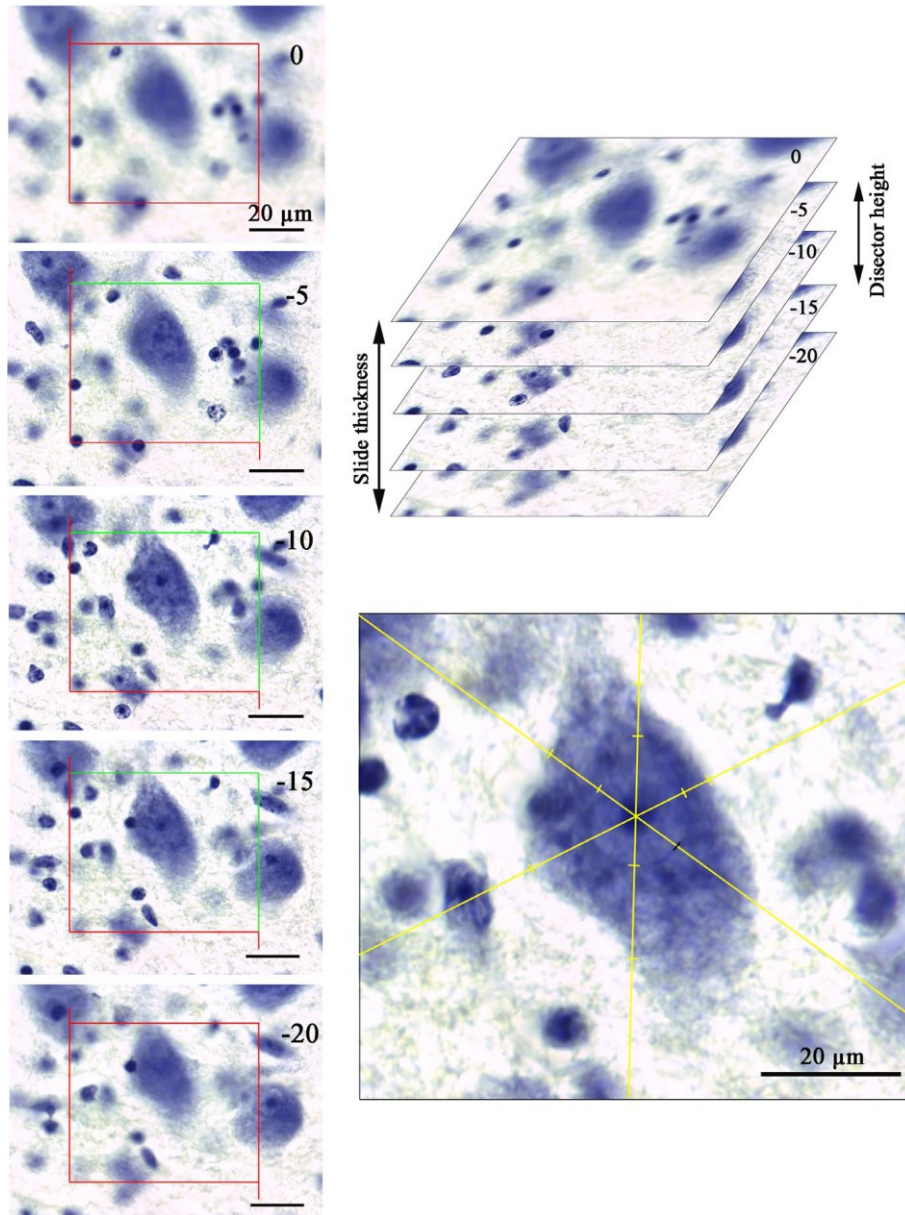


**Figure 3.** Use of the optical disector technique for the Purkinje cell count and of the nucleator technique for the estimation of the Purkinje cellular and nuclear volumes. **(a):** The microscopic fields were selected by moving the microscope stage in the x and y directions for a constant distance. Then, the stage of microscope moved in z-axis and the consecutive focal planes were evaluated within optical disector height (10 μm from -5 to -15 μm).

(b-f): The unbiased counting frame principle was applied for the Purkinje cell count. The cells whose nucleolus was located inside the counting frame or crossed the accepted lines were sampled, and those whose nucleolus came into focus within disector height were counted. (g): The intercept length from the nucleolus to the border of the cytoplasm, or to the border of the nucleus, was measured for the estimation of Purkinje cellular and nuclear volumes, respectively.

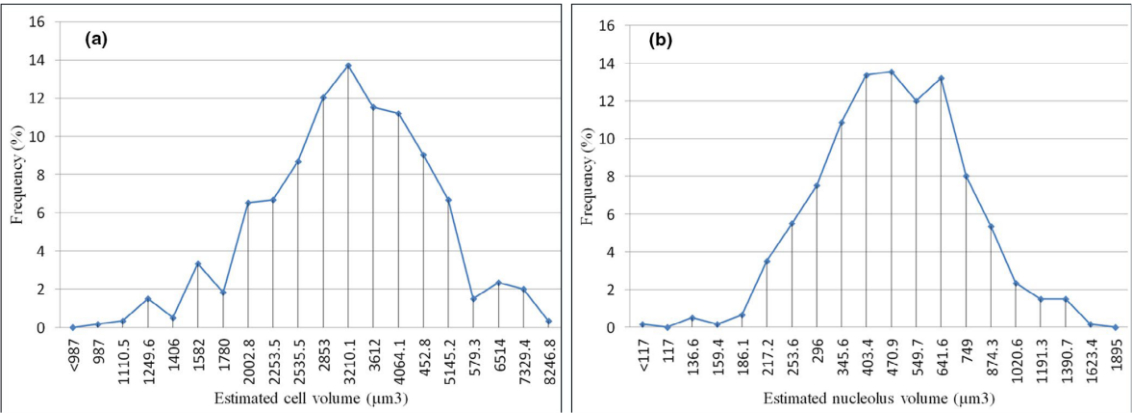


**Figure 4.** Graphs showing the frequency distribution of the Purkinje cellular (a) and nuclear (b) volumes in the guinea-pig cerebellum.